Reliable CFD-based estimation of flow rate in haemodynamics measures

R. Ponzini[1,2], C. Vergara[3], A. Redaelli[1], A. Veneziani[3]

30th January 2006

1-Department of Bioengineering, Politecnico di Milano, Italy
2-CILEA (Consorzio Interuniversitario Lombardo per l'Elaborazione e l'Automazione), Segrate (MI), Italy
3-MOX (Modeling and Scientific Computing) - Department of Mathematics, Politecnico di Milano, Italy

Keywords: Flow rate estimation, Doppler technique, Computational Fluid Dynamics, flow rate boundary conditions, Womersley number.

AMS Subject Classification: 62G99

Abstract

Physical useful measures in current clinical practice refer often to the blood flow rate, that is related to the mean velocity. However, the direct measure of the latter is currently not possible using a *Doppler* velocimetry technique. Therefore, the usual approach to calculate the flow rate with this technique consists in measuring the maximum velocity and in estimating the mean velocity, making the hypothesis of parabolic profile, that in realistic situations brings to strongly inaccurate estimates.

In this paper, we propose a different way for estimating the flow rate regarded as a function of maximum velocity and *Womersley number*. This relation is obtained by fixing a parametrized representation and by evaluating the parameters by means of a least square approach working on the numerical results of CFD simulations (about 200). Numerical simulations are carried out by prescribing the flow rate, not the velocity profile. In this way, no bias are implicitly induced in prescribing boundary conditions. Validation tests based on numerical simulations show that the proposed relation improves the flow rate estimation.

1 Introduction

The correct knowledge of the blood flow rate Q in a vascular district is a major issue in many clinical situations for estimating the perfusion state of a certain

tissue and for decision-making when a cardiovascular disease occurs. For example, the evaluation of the flow reserve, defined as the ratio between the maximal flow obtained in vasodilation conditions and the baseline conditions, is one of the most important parameters used to characterize the haemodynamics impact of a luminal obstruction. If Γ denotes a section of the vascular district at hand, the flow rate Q through Γ is given by:

$$Q = \int_{\Gamma} \rho \boldsymbol{v} \cdot \boldsymbol{n} d\gamma \tag{1}$$

where ρ is the blood density, $\boldsymbol{v}$ the velocity and $\boldsymbol{n}$ the normal unit vector. In principle the knowledge of the whole velocity field on Γ is needed for the computation of Q. However, this information cannot be obtained in ordinary Doppler velocimetry analysis. A different way for representing Q is to resort to a *mean velocity* value $\widetilde{V}$ such that

$$Q(t) = \rho \widetilde{V}(t) A(t), \tag{2}$$

where A is the measure of Γ. The problem with this formulation is still that $\widetilde{V}$ cannot be directly measured, therefore it is currently estimated by the measure of the maximum value of velocity V_M on Γ by means of an appropriate relation linking V_M to $\widetilde{V}$. In particular, it is usually assumed (see Doucette et al. 1992) that

$$\widetilde{V} = \frac{1}{2} V_M. \tag{3}$$

This equation stems from the hypothesis of a *parabolic* spatial profile for the velocity. According to this assumption, blood is considered a steady, laminar Newtonian fluid in a cylindrical vessel (see e.g. Nichols and O'Rourke 1990). In real situations, blood flow is far from fulfilling these features. Several works (see e.g. Robertson et al. 2001, Perktold et al. 1998, Sheada et al. 1993, Ponzini et al. 2006) pointed out that a non parabolic profile can be computed in simulating realistic conditions even when the considered morphologies were the same of those studied in the validation protocol of the Doppler guide wire (see e.g. Doucette et al. 1992, Savader et al . 1997).

In particular, the relevance of blood pulsatility on velocity profiles has been clearly pointed out since a long time by Womersley (1955) and among the others, we quote Hale et al. (1955) and Nichols and O'Rourke (1990). These works highlight that the hypothesis that blood is quasi-static (i.e. that at each instant the velocity profile is the same as for a steady fluid featuring the flow rate prescribed at that instant) is not realistic, in particular when the *Womersley number* $W = r\sqrt{2\pi f/\mu} = \sqrt{2Af/\mu}$ (where $r = \sqrt{A/\pi}$ is the vessel radius, f the frequency of blood impulse and μ the blood viscosity) increases. The limited validity of the parabolic profile assumption has been clearly pointed out also in Jenni et al. (2000 and 2004) and in Porenta et al. (1999). In these works, the authors found that the use of (3) to estimate the mean velocity value is too

simplistic and can lead to misleading results in the coronary CFR (Coronary Functional Reserve) evaluation of the flux. Starting from this observation, they propose to modify the acquisition procedure at the operator's level according to the Hottinger and Meindl principle (see Hottinger and Meindl 1979).

In order to obtain a more realistic relation linking V_M to $\widetilde{V}$ taking into account the pulsatility of the blood flow rate, a first possibility is to utilize the analytical relationship that He et al. (1993) proposed for a cylindrical domain for a sinusoidal signal. This approach can be extended to general physiological waveforms by application of the superimposition effects principle that holds for linear problems. However, this approach has two major drawbacks. On one hand it has been devised for cylindrical morphologies and its extension to more realistic geometries seems not trivial and somehow problematic. On the other one, the problem at hand is driven by the non-linear Navier-Stokes equations, so the superimposition of effects is strictly non applicable. When the Reynolds number increases, that means that the non linearity becomes more relevant, this can induces some inaccuracies. For these reasons, alternatively some works developed different relations between the maximum and the mean velocity, using Computational Fluid Dynamics (CFD) for specific cases. In this context, approximations have been found by Pennati et al. (1996 and 1998) for the case of the ductus venosus and by Ponzini et al. (2006) for coronary Y-graft bypass.

In the present work, we propose an "operator independent" approach, based on CFD, for improving blood flow estimates from maximum velocity measures that basically relies on the *mean velocity/vessel area method* (consisting in measuring the lumen area and the maximum value of velocity and in computing the mean velocity as a function of this value) and on a generalization of (3). In principle, we could think to extend this formula by introducing a relation of the form

$$\widetilde{V} = g(V_M, r, f, \mu, \ldots),$$

where all significant parameters (such as the vessel curvature or torsion) can be included for improving the accuracy of the mean velocity. However, the management in the clinical practice of all these parameters could be somehow problematic and even unnecessary. We decide therefore to select only one significant parameter besides the maximum velocity. As a matter of fact, we introduce the relation

$$\widetilde{V} = g(V_M, W), \tag{4}$$

establishing a link between the $\widetilde{V}$ (and then the flow rate) and V_M as a function of the Womersley number W summarizing in a synthetic way some geometrical, fluid dynamical and rheological features. Function g will be fixed by specifying some parameters, depending on its specific functional form. The quantitative determination of these parameters can be carried out by fitting available data with a least squares approach. These data could be provided by "in vitro" measures taken in realistic experimental set up. Alternatively, fitting can be carried out by exploiting numerical simulations (see Pennati et al. 1998 and Ponzini et al.

2006). So far, haemodynamics computations with flow rate boundary conditions have been carried out by specifying an arbitrary velocity profile. The reason of this is that from the mathematical viewpoint flow rate boundary conditions are not enough to have a well posed problem and the available conditions are completed by selecting a velocity profile compatible with the prescribed flow rate. In the context of the present work, the prescription of a velocity profile would be equivalent to select *a priori* for each value of W a functional relation like (4) and this would reduce the significance of numerical simulations (see Redaelli et al. 1997) and definitely the accuracy of (4) in recovering the flow rate from the maximum velocity. Recently, new numerical techniques have been however devised for solving haemodynamics flow rates problems *without* the prescription of a velocity profile (see Heywood et al. 1996, Formaggia et al. 2002, Veneziani and Vergara 2005a). The potential bias in using numerical simulations specifying the velocity profile can be therefore avoided. Several accurate numerical simulations in different realistic situations have been therefore carried out for collecting data useful for the least squares estimate of the parameters in (4). By so doing, we firstly derive two different equations in the form (4) well suited for representing the link between V_M and $\widetilde{V}$ for two different representative groups of vessels. Afterwards, by an appropriate combination of these formulae, we obtain a unique equation covering different geometrical features and a physiological range of Womersley numbers.

The effectiveness of the formula has been validated by resorting again to numerical simulations. By computing blood flow in geometries and conditions different than the ones used for the least squares fitting, we observed that our formula yields a (sometimes *strong*) improvement of the flow rate estimation based on the (3). We think therefore that this result can be potentially of big interest in clinical practice. However, successive *in vitro* and *in vivo* validation to confirm the present study are mandatory.

The outline of the paper is as follows. In Section 2 we present the basic features of model (4). We firstly present models used for the two significant groups of vessel and give details about the least squares fitting. We avoid mathematical details about CFD methods for getting reliable numerical simulations, referring the interested reader to Formaggia et al. (2002) and to Veneziani and Vergara (2005a). Then, we illustrate how the two formulae have been collected in a unique equation of the form (4). Validation is presented in Section 3. Conclusions and perpectives are drawn in Section 4.

2 Materials and Methods

2.1 Basic features of the mathematical model

The specific features of the flow patterns in a vascular district, once boundary conditions have been assigned, are basically the morphology, the pulsatility and the rheology. On one hand, one would set up an accurate equation linking the

mean and the maximum velocities, taking into account all these aspects. On the other hand, the usage of this equation is subordinated to the possibility of getting reliable estimates of all these features in the clinical practice. As pointed out in the Introduction, as a reasonable compromise between the accuracy and the feasibility, we summarize the dependence on all these features by resorting to the Womersley number (see equation (4). In this way, we synthetically account for the radius of the vessel, the blood viscosity and in particular for the *pulsatility*. W can be in practice estimated on the basis of available clinical measures. We actually are assuming that it is possible to define locally a *vessel radius*. This will be the only geometrical parameter in our equation. More complex (and more difficult to implement) equations could be considered in a future development of the present work.

The direct derivation of a unique, exhaustive formula for the estimation of the flow rate in the whole Womersley number physiological range, would be optimal from the operative point of view. Nevertheless, we found that the fitting procedure brought to an inaccurate unique formula. Therefore, for the sake of accuracy, we decided to consider two different situations representative for small and medium/large vessels (see Figure 1) and to devise for each one a different equation (4). We address separately one computational protocol in each case.

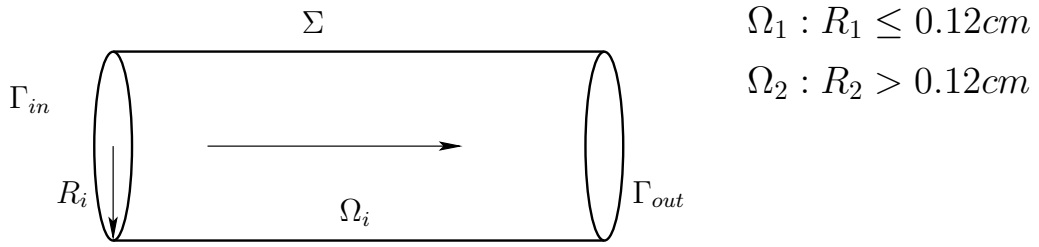

Figure 1: Reference domains Ω_i.

2.1.1 Small vessels

Small vessels are represented by a cylindrical domain Ω_1 with $R_1 \leq 0.12cm$. In this class of vessels, a physiological range for the Womersley number is (see Nichols et al. 1990, Wells 1970, Bloch and Maki 1973, Wolthuis et al. 1997):

$$W \leq 3.1.$$

A possible general formulation for the equation (4) to be used in the case of small vessels is:

$$\widetilde{V} = g_1(V_M, W) = \frac{1}{2} V_M \left(1 + a_1 W^{b_1}\right), \tag{5}$$

where a_1 and b_1 are the parameters to be fitted. This parametric representation has been selected as a power law generalization of the steady ($W = 0$)

equation (3). In the numerical simulations carried out for fitting a_1 and b_1, we distinguished two situations that can be referred to "small vessels":

1. small arteries
2. coronaries.

The two cases are considered separately because, as it is well known, the flow rate waveform in the coronaries is by far different than the one in the other small arteries due to the heart squeezing. This actually means that in the fitting procedure we selected two different set of test cases adopting two different flow rate waveforms. In particular, for small arteries we choose the profile reported in Figure 2, left, representing the flow rate in the *vertebral artery*, following Viedma et al. (1997). For the coronary fitting, waveform is reported in Figure 2, right, taken from Perktold et al. (1998).

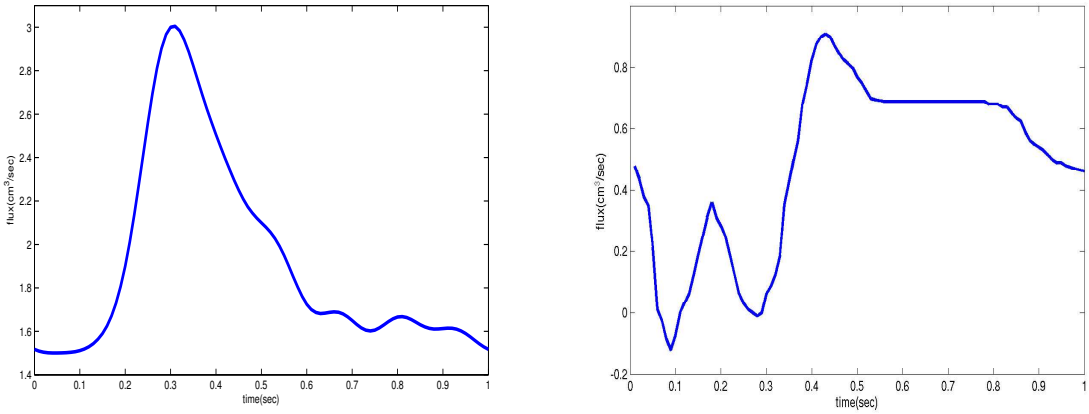

Figure 2: Vertebral (left) and coronaric (right) flow waves with $f = 1\,Hz$ imposed in Ω_1

2.1.2 Medium/Large vessels

Medium and large vessels are represented by a value of radius $R_2 > 0.12$ cm in the Womersley number range (see Nichols et al. 1990, Wells 1970, Bloch and Maki 1973, Wolthuis et al. 1997):

$$2.70 \leq W \leq 15.$$

In this case, we found that an appropriate parametric representation of (4) is:

$$\widetilde{V} = g_2(V_M, W) = \frac{1}{2} V_M b_2 \arctan(a_2 W), \tag{6}$$

being a_2 and b_2 the parameters again. In order to fit the parameters, we used the flow rates in Figure 3, representing the flux in the *iliac* and in the *aortic* artery respectively (see Olufsen et al. 2000).

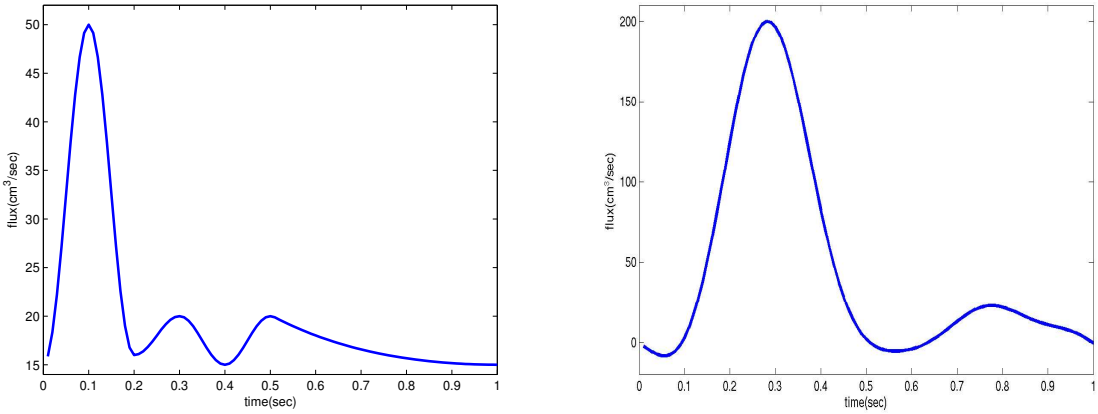

Figure 3: Iliac (left) and aortic (right) flow waves with $f = 1\,Hz$ imposed in Ω_2

2.2 The Fitting Procedure

For each of the considered situations (small and medium/large vessels), parameters can be fitted if several estimates of data in the form (V_M, W) are available. These data can be collected sperimentally or computed numerically (CFD). In this work, we pursued the second approach. In particular, since we aim at setting up a computational protocol similar to the clinical one, in which V_M is the maximum velocity in space and in time, we focus our attention on the peak velocity instant (see Figure 4). Data for the fitting are taken at that instant. Since we are assuming vessels can be reasonably considered rigid, it is worth observing that in (2) A is constant-in-time, so the computation of the flow rate Q on a section Γ from the mean velocity $\widetilde{V}$ is done by

$$Q(t) = \rho \int_\Gamma \boldsymbol{v} \cdot \boldsymbol{n} d\gamma = \rho A \widetilde{V} \quad \forall t \in (0, T), \tag{7}$$

where the density ρ is assumed constant.

Blood has been simulated as an incompressible fluid in a rigid vessel fulfilling the well known set of Navier-Stokes equations (see e.g. White 1987):

$$\begin{cases} \rho \dfrac{\partial \boldsymbol{v}}{\partial t} - \mu \triangle \boldsymbol{v} + \rho(\boldsymbol{v} \cdot \nabla)\boldsymbol{v} + \boldsymbol{\nabla} P = \rho \boldsymbol{f} \quad \text{in} \quad \Omega \times (0, T) \\ \operatorname{div} \boldsymbol{v} = 0 \quad \text{in} \quad \Omega \times (0, T) \\ \boldsymbol{v}(\boldsymbol{x}, 0) = \boldsymbol{v}_0(\boldsymbol{x}) \quad \text{in} \quad \Omega, \end{cases} \tag{8}$$

where P the pressure, $\boldsymbol{v}_0$ a given initial datum and $\boldsymbol{f}$ a given forcing term. Equations (8) have to be completed with suitable boundary conditions. In particular, we impose a *no-slip* condition on the physical wall Σ (i.e. $\boldsymbol{v}|_\Sigma = \boldsymbol{0}$), corresponding to the assumption of rigid walls, and null normal stress on the outlet Γ_{out}. On the inlet, we prescribed the flow rate (1) specified by the waveforms reported in Figures 2 and 3.

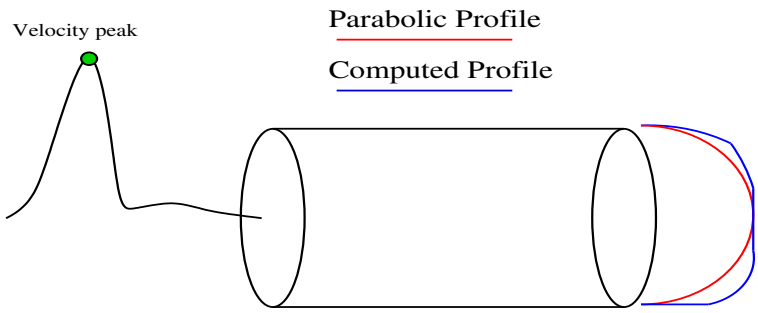

Figure 4: Overall vision of the computational protocol: at the peak instant the comparison between the parabolic profile and the computed is done in order to evaluate and correct the flux estimation.

From the mathematical viewpoint, these boundary conditions are not sufficient to have a well posed problem. Typically, in haemodynamics simulations this lackness of data is overcome by selecting a velocity profile (possibly far away from the region of interest) compatible with the available flow rate data (see Pennati et al. 1996 and 1998). In the present contex, this approach is not feasible, since the prescription of an arbitrary velocity profile would affect the parameter quantification in (5) and (6) and definitely the flow rate estimates. Recently, a mathematically more sound approach for solving flow rate problems without the prescription of a velocity profile has been proposed in Formaggia et al. (2002) and investigated in Veneziani and Vergara (2005a and 2005b). The basic idea is to consider (1) not as a boundary condition but as a *constraint* for the solution. The fulfillment of this constraint can be forced by means of a *Lagrange multiplier approach*. The drawback of this approach is that the computational cost can be strongly increased due to the computation of the Lagrange multipliers (see Veneziani and Vergara 2005b). On the other hand, numerical simulations show that this formulation of the problem yields more realistic numerical results (see Veneziani and Vergara 2005a) . For the numerical results of the present paper, the Finite Element Library `lifev` (see `www.lifev.org`) has been used. However, we point out that also commercial packages can be suitably adapted for solving non-standard flow rate boundary problems (see Veneziani and Vergara 2005a and 2005b).

We solved the Navier Stokes equations in a computational domain like the one showed in Figure 1 (using $R_1 = 0.06, 0.12$ cm and $R_2 = 0.24, 0.4, 0.5, 0.7$ cm) for a total of 182 simulations in the range of W illustrated in Figure 5. Simulation parameters (viscosity and frequency) have been varied in order to perform two simulation for each imposed flow rate (see Section 2.1) at each W; in particular the blood viscosity changes in this discrete set $(0.022, 0.03, 0.035, 0.04)$ Poise according to Bloch and Maki (1973) and Wells (1970), while the frequency in the range $(0.6, 3)$ Hz according to Wolthuis et al. (1997). Once large data set made of vectors of evaluations (V_M, W) for the prescribed Q are available

from numerical simulations, parameters in (5), (6) are obtained by means of a non-linear least-square fitting optimization. In particular, we have used the Least Squares module present in the package Scientific-Python. We do not dwell here with further mathematical details. The interested reader is referred to Langtangen (2004).

2.3 A unified approach

More data can be included in tuning parameters in (4) and more accurate will be the estimates obtained. In particular, this means that if we restrict the range of validity of (4) to specific situations and perform specific parametric fittings, we will obtain a set of equations very accurate for the situations they are devised for. The two formulae (5) and (6) will be therefore very accurate in the appropriate range of Womersley numbers (see Section 3.1). In principle, more accuracy could be achieved by furtherly specializing the validity of each formula. For instance, by separating the fitting for small arteries and coronaries, two set of parameters would be obtained for equation (5), each of them seemingly very accurate for the case of small arteries and coronaries respectively. The drawback is however that, in practice, it could be difficult to manage three, four (or even more) different equations for estimating the flow rate. A unique formula will be less accurate but easier to use in the clinical practice. For this reason, after considering the two cases presented above seprately, we devised a unique formula spanning the whole range of phyisological Womersley numbers. The set up of a unique formula can be achieved in different ways. Here we simply decided to introduce a suitable weighted linear combination of the two functions $g_1(V_M, W)$ and $g_2(V_M, W)$. More precisely, in presenting the two cases considered we introduced an overlapping subdivision of the range of Womersley numbers (see Figure 5). Hereafter, we will say that a function g_i $(i = 1, 2)$ is "active" on an interval of this subdivision, if it has been set up in a Womersley numbers range including that interval.

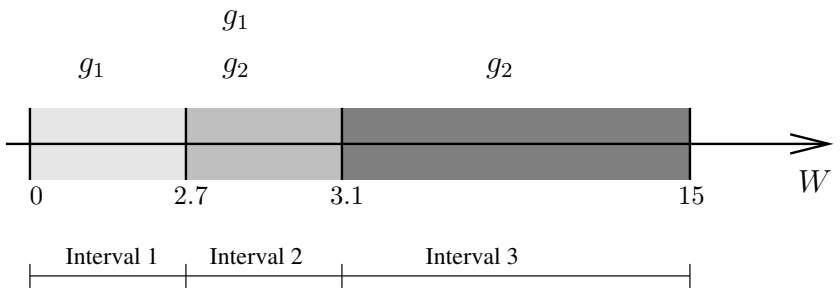

Figure 5: Subdivision of the whole range of Womersley numbers into intervals with the specification of the different active g_i $(i = 1, 2)$.

We have therefore the following subdivision:

Interval 1 For $W < 2.70$ the only active function is g_1;

Interval 2 For $2.70 \leq W < 3.1$ the active functions are both g_1 and g_2;

Interval 3 For $3.1 < W \leq 15$ only g_2 is active.

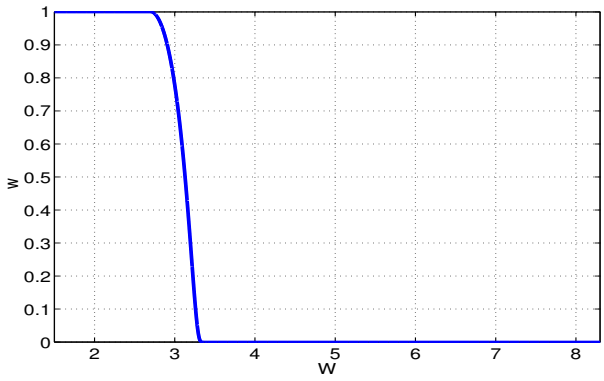

Figure 6: Weight function w

A unified function g can be therefore obtained by forcing g to be equal to the only active function in the Intervals 1, 3 and to a linear convex combination of the two active functions on the Interval 2. This means that we set:

$$\widetilde{V} = g(V_M, W) = \begin{cases} g_1 & W \leq 2.7 \\ wg_1 + (1-w)g_2 & 2.7 < W \leq 3.1 \\ g_2 & 3.1 < W \leq 15 \end{cases} \tag{9}$$

The weight function $w(W)$ is represented in Figure 6: it is infinitely smooth function equal to 1 on the left end point of Interval 2 and 0 on the right one, given by:

$$w = e^{\frac{(W-2.7)^2}{(W-2.7)^2-(3.1-2.7)^2}}.$$

Equation (9) is the formula of the class (4) we are going to validate in the next Section.

3 Results

The fitting procedure for the two cases considered in Section 2 leads to the following estimates of the parameters in (5) and (6):

$$\begin{cases} a_1 = 0.00417, & b_1 = 2.95272 \\ a_2 = 1.00241, & b_2 = 0.94973 \end{cases} \tag{10}$$

The performances of (5), (6) and (9) with parameters given by (10) have been tested in three cases. In the first one, we referred to the same conditions used for fitting the parameters, as a consistency test of the least square

approach adopted for the parameters estimation. In the second test cases set, we retained the same geometries used for the parameters fitting and changed the inlet flow rate waveforms used. In the last class of benchmarks, we applied (9) to completely different geometries and flow rate waveforms. In each case, we compare the mean velocity estimated by (5), (6) or (9) with (10), starting from the outlet maximum velocity, with the exact prescribed value and with the parabolic estimate (3). Finally, in order to compare our new method with the parabolic one, we applied the Bland-Altman test (see Bland and Altman 1986) to the validation test cases described in Section 3.2 and 3.3. This statistical test is usually performed in clinical practice to evaluate the level of agreement of a new measurement technique with an established one.

3.1 A consistency test

In Figures 7 and 8 we report the relative errors on the flow rates estimated by (5), (6), (9) with (10) and by (3), when using the results of the numerical simulations described in Section 2. As was to be expected in this favorable case, in which the haemodynamics conditions do actually coincide with the one used for the fitting, the improvement induced by the new formulae is relevant for all the cases considered.

It is worth pointing out that the accuracy of the estimate based on (9) reduces in the Interval 2 (see Figure 5) where the two functions g_1 and g_2 are both active, in particular with respect to the corresponding estimate given by the g_i alone in the associated intervals. This is still to be expected, since for the specific case in which a function g_i has been devised it works obviously better. In fact, the unified formula in this range does not show a significant improvement with the respect to (3).

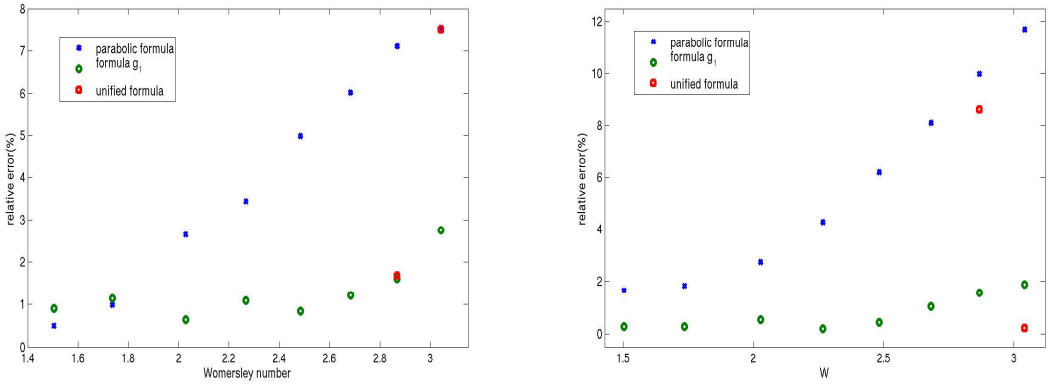

Figure 7: Relative errors between the estimated fluxes and the imposed ones for the geometry Ω_1 with the vertebral (left) and the coronary (right) flow waves.

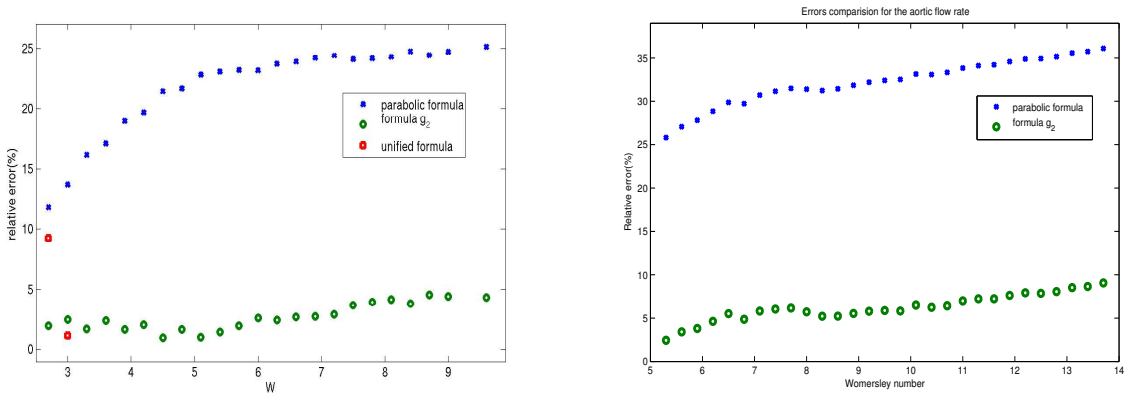

Figure 8: Relative errors between the estimated fluxes and the imposed ones for the geometries Ω_2 with iliac (left) and by the aortic (right) flow rate.

3.2 Different waveforms

In this benchmark, we decided to maintain the same geometries as for the parameters fitting, and to simulate different waveforms for the perfusing flow rate. We compare the fluxes estimated by (9) with (10) and by (3) with the exact prescribed flow rate. In particular, we firstly imposed the flow wave reported in Figure 9, found in a proximal LITA (Left Interior Thoracic Artery) used as an aorto-coronary by-pass, at the inlet of a domain Ω_1 with radius equal to 0.12 cm (see Ponzini et al. 2006).

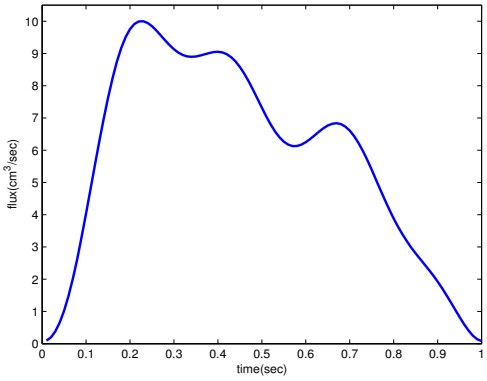

Figure 9: Proximal LITA inlet flow rate waveform

Secondly, we imposed the physiological flow rate perfusing the *renal artery* reported in Figure 10, left, at the inlet of a domain Ω_2 with radius equal to 0.4 cm (see Nichols and O'Rourke 1990). Then, we imposed the physiological flow rate perfusing the *brachialis artery* reported in Figure 10, right, at the inlet of a

domain Ω_2 with radius equal to 0.24 cm (see Olufsen et al. 2000). In Table 1 we report the relative errors introduced by the two formulae in these three cases.

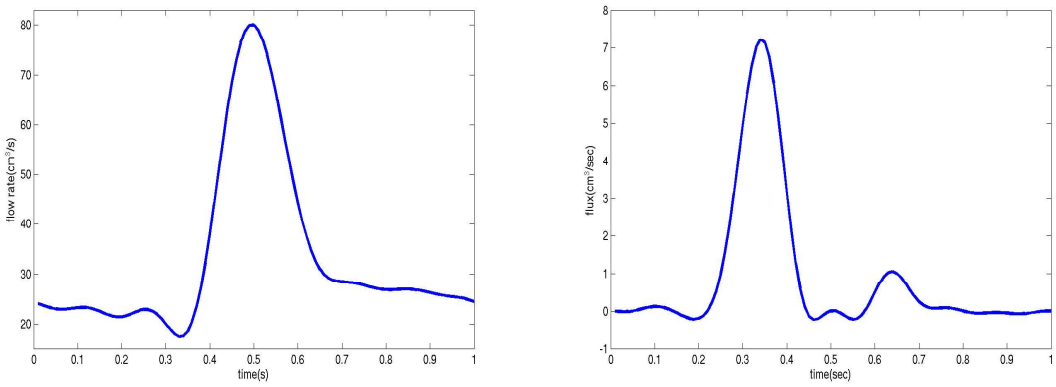

Figure 10: Renal and brachialis inlet flow rate waveforms

	W	Estimate based on (3)	Estimate based on (9)
Proximal LITA	1.7366	1.24%	0.86%
	2.2673	4.20%	0.28%
	2.868	9.09%	3.64%
	3.0419	9.64%	6.68%
Renal	5.3594	18.34%	4.12%
	7.5793	23.64%	4.43%
	8.8676	25.38%	3.38%
Brachialis	2.868	18.42%	9.29%
	3.0419	18.17%	1.32%
	5.3594	32.50%	11.09%
	7.5793	38.34%	15.67%

Table 1: Relative errors for the proximal LITA, renal and brachialis flow wave test case.

We point out that in four of the eleven cases the Womersely number is in Interval 2, Figure 5, where the unified formula differs from g_1 and g_2. The improvement introduced by the new formula is still relevant.

3.3 Different geometries and waveforms

In this validation test we refer to the numerical results obtained in a realistic carotid model reported in Figure 11, obtained from real data of a patient through a cast produced by D. Liepsch - FH Munich. This geometry is by far different from the cylindrical morphologies used for the parameters assessment.

We prescribe the physiological flow rate shown in Figure 12 both at the inlet and at the internal outlet of the carotid (see Fig. 11).

In Figure 11 - right, the velocity field at the peak systolic instant is shown. The results in Table 2 show that the relative errors in estimating the flux from the maximum velocity using (9) with (10) are really less than the estimates based on (3).

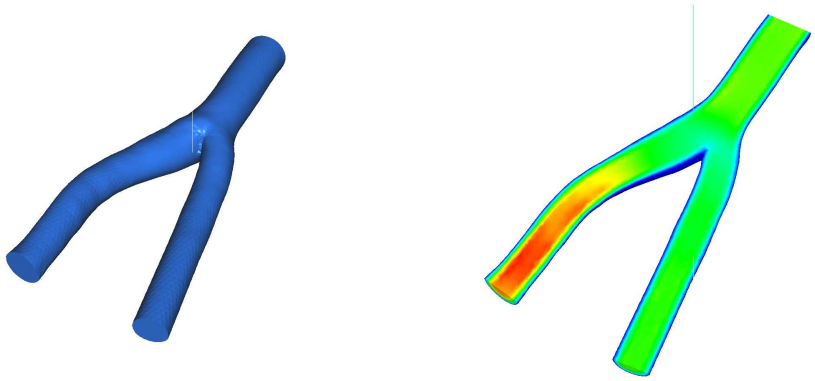

Figure 11: Carotid domain (left) and velocity field (right)

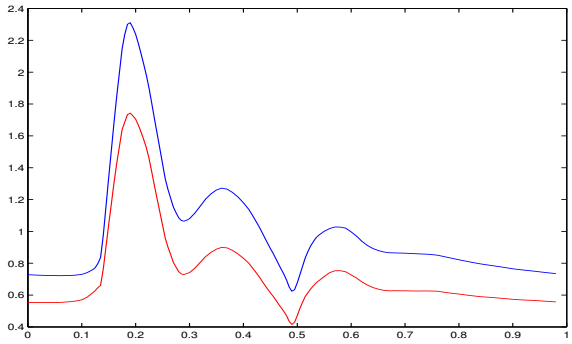

Figure 12: Imposed flow rates at the inlet (blue line) and at the internal outlet (red line) in the carotid ($\times 50 cm^3/sec$)

3.4 Bland-Altman test

We tested the value of the imposed flow rate (Q_I) as the golden standard against the value of the flow rate estimated using equation (3) (Q_D) and using equation (10) (Q_W), respectively, for the validation test cases presented in Section 3.2 and 3.3. Figure 13 reports the differences plotted against their average, within

	Inlet	Outlet I	Outlet II
W	7.74	5.21	4.90
Radius (cm)	0.5	0.337	0.317
$V_{peak}\,(cm/sec)$	204.47	339.55	132.15
Imposed flux (cm^3/sec)	115.33	86.97	28.36
Relative error with parabolic formula (%)	31.27	30.56	26.69
Relative error with correction formula (%)	4.61	8.88	4.62

Table 2: Application of (9) in a numerical model of carotid bifurcation

two standard deviations from the mean difference between Q_I, Q_D and Q_I and Q_W, respectively. The range obtained represents the 95% confidence interval of the two computed differences. The results obtained testing Q_I versus Q_D show clinically important differences with the presence of a consistent bias ($bias = 9.48 \pm 11.51\, ml/s$). On the contrary the differences testing Q_I versus Q_W present a less significant bias ($bias = 1.95 \pm 2.31\, ml/s$) and therefore Q_W provide a more suitable estimate of Q_I.

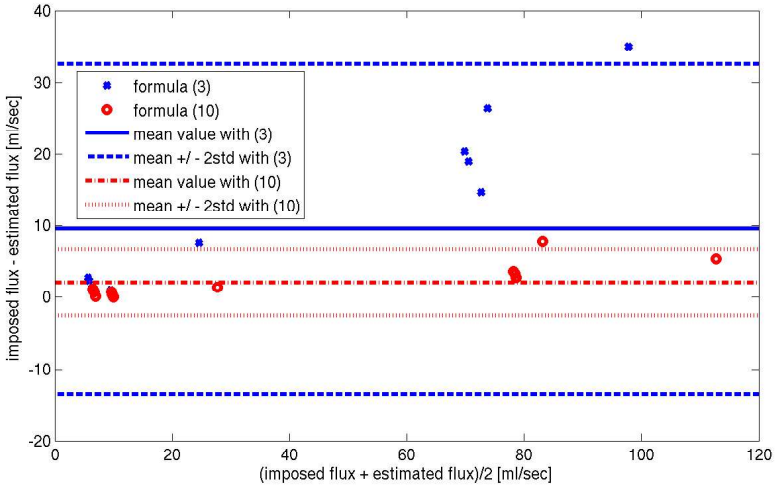

Figure 13: Bland-Altman test for Q_I versus Q_D and Q_W.

4 Discussion and Conclusions

The problem of extracting reliable informations on the blood flow volume starting from velocimetry data acquisition is of utmost importance in haemodynamical measures. Several (geometrical, fluid dynamical, operator-dependent) degrees of uncertainty are present in such a procedure and they could be a source

of bias and/or random errors.

In this work we have presented how the extensive use of numerical simulations can enhance currently in use procedures, based on analytical solutions of the flow field like the Poiseuille one. Actually, some of the hypotheses assumed for analytical solutions can be removed thanks to numerical simulations, yielding definitely better estimates of relevant quantities starting from velocimetry data. In particular, in the present work, we removed the unrealistic parabolic assumption implicitly introduced in (3) for the flow rate estimates from maximum velocity measures. In devising new relations for the blood flow estimate, we therefore chose the Womersley number as a measure of the fluid unsteadiness. Numerical simulations have provided data for the fitting of the parameters selected in the specification of the new formula. The data collection has been firstly differentiated into two representative cases, corresponding to small and medium/large vessels, and then a unique equation (9) has been computed by linear combination.

Using CFD for this aim has many advantages:

1. The so called *mean velocity/vessel area method* used in velocimetry data acquisition can be accurately reproduced;

2. Simplifying assumptions present in previous methods can be removed in a controlled manner, possibly identifying the most relevant ones;

3. Collection of data for the parameters fitting is quite fast and cheap;

4. Validation and benchmarking can still be based (at least partially) on numerical simulations carried out in configurations different form the ones used for the fitting.

5. The previous advantages are related to general CFD. Moreover, in our particular case, we point out that the prescription of the flow rate boundary condition without prescribing a priori the velocity profile through a Lagrange multipliers approach, leads to meaningful numerical results avoiding the bias induced by the prescription of the inlet velocity profile.

The results obtained by our formula show clearly the systematic incorrectness of the parabolic hypothesis used in daily clinical velocimetry analysis. The relative error of the parabolic formula increase with the Womersley number. More precisely, it is worth pointing out that:

1. The relative error associated with the parabolic prediction formula (3) in the consistency test (Section 3.1) shows a systematic underestimation (mean = 22.01%, stdv = 11.08%) ;

2. The relative error associated with the prediction formula (9), in the consistency test, is bounded in a very small range as a consequence of the accounting for the pulsatile nature of blood (mean = 3.73%, stdv = 2.51%);

3. The magnitude of the error using (3) depends on the shape of the waveform perfusing the vessel. The same does not seem to hold for (9) (see Figure 7 and 8). Hence, formula (9) seems to be robust with respect to the shape of the flow rate. Moreover, we point out that in the range of W corresponding to Interval 2, Figure 5, formulae (5) and (6) are better than (9). Nevertheless, the latter is easier to implement.

4. The choice of cylindrical domain for building formula (9) and for testing its validity versus (3) (Section 3.2) has been done in order to isolate the effect of pulsatility on the velocity profile. However, we point out that this approach can be extended in order to build new formulae taking into account different (realistic) geometries.

5. The application of this correction procedure in the specific computational model of carotid bifurcation (Section 3.3) improves the blood flow volume prediction (see Table 2). In particular the error in the three sections reduces from more than 30% to less then 10%.

6. The test of Bland-Altman confirmed that the use of equation (9) as a measurement technique provides an higher level of agreement with the imposed value of the flow rate rather than the one provided by using equation (3) (see Fig. 13). We point out that the value of the bias using (9) is $1.95\, ml/sec$ versus $9.48\, ml/sec$ obtained using (3) and that the 95% confidence interval associated is significantly smaller in the former case.

There are many directions for improving the present work.

1. On one side, we can remove some simplifying assumptions made in order to build a formula like (4); for instance, simulations in curved pipes or with compliant walls could be carried out for a finer or more specific formula.

2. Another possibility is to introduce new independent variables in the relation between the maximum and the mean velocities, beyond the Womersley number. For instance, one could account here for the possible curvature k or other morphological features, by devising a formula in the form:

$$\widetilde{V} = g(V_M, W, k, ...).$$

   Other, more complicates, independent variables can be chosen in this context, with the constraint that they should be (easily) measurable in order to be used for a real-time estimates of the flow rate.

In this sense the general approach presented in this paper is trainable, adaptable and customizable to take into account specific (maybe pathological) clinical scenarios at all level (geometry, rheology, fluid dynamics, etc.). In conclusion, we can state that in the Poiseuille hypothesis, a significant component of bias is present, while using the proposed formula (9), this error can be significantly

reduced. An extensive "in vitro" and "in vivo" validation activity is now mandatory as a necessary phase for confirming the strong improvements found here, before incorporating this formula into clinical devices.

Acknowledgments

Numerical results of this work have been obtained with the finite element codes LifeV (developed at MOX - Dipartimento di Matematica - Politecnico di Milano, at EPFL in Lausanne and at INRIA at Paris, see `www.lifev.org`)). The authors gratefully acknowledge M. Prosi who provided the bifurcation computational domain and in particular G.Pennati at *Laboratory of Biological Structure Mechanics (LaBS), Politecnico di Milano*, for many friutful discussions and suggestions.

References

[1] Bland J.M., Altman D.G., Statistical methods for assessing agreement between two methods of clinical measurement,*Lancet*; **1**(8476):307-310, 1986.

[2] Bloch K.J. and Maki D.G., Hyperviscosity syndrome associated with immunoglobulin abnormalities, *J. Sem. Hematol.* ;**10**:113126 , 1973.

[3] Doucette J.W., Corl P.D., Payne H.M., Flynn A.E., Goto M., Nassi M., Segal J., Validation of a Doppler guide wire for intravascular measurement of coronary artery flow velocity, *Circulation*; **85**, 1899-1911 , 1992.

[4] Formaggia L., Gerbeau J.F., Nobile F., Quarteroni A., Numerical treatment of Defective Boundary Conditions for the Navier-Stokes equation, *SIAM J. Num. Anal.*; **40**(1):376-401, 2002

[5] Hale J.F., McDonald D.A., Womersley J.R., Velocity profiles of oscillating arterial flow, with some calculations of viscous drag and the Reynolds numbers, *J. Physiol.*; **128** (3):629-40 1955.

[6] He X., Ku D.N., Moore J.E. Jr, Simple calculation of the velocity profiles for pulatile flow in a blood vessel using *Mathematica*, *Ann. Biomed. Eng.*; **21**, 45-49,1993.

[7] Heywood, Rannacher and Turek, Artificial Boundary and Flux and Pressure Conditions for the Incompressible Navier-Stokes Equations, *Int. Journ. Num. Meth. Fluids*; **22**, 325-352,1996.

[8] Hottinger C.F., Meindl J.D., Blood flow mesaurements using the attenuation-compensated volume flowmeter, *Ultrasound Imaging*; **1**(1):1-15, 1979.

[9] Jenni R., Kaufmann P.A., Jiang Z., Attenhofer C., Linka A., Mandinov L., In vitro validation of volumetric blood flow measurement using Doppler flow wire, *Ultrasound Med Biol.*; **26**(8):1301-10, 2000.

[10] Jenni R., Matthews F., Aschkenasy S.V., Lachat M., van Der Loo B., Oechslin E., Namdar M., Jiang Z., Kaufmann P.A., A novel in vivo procedure for volumetric flow measurements. *Ultrasound Med Biol.*; **30**(5):633-7, 2004.

[11] Langtangen H. P., *Python Scripting for Computational Science*, Springer, 2004.

[12] Nichols W.W., O'Rourke M.F. , *McDonald's blood flow in arteries*, (V Ed.), Hodder Arnold (Eds.), 1990.

[13] Olufsen M.S., Peskin C.S., Kim W.Y., Pedersen E.M., Nadim A., Larsen J., Numerical Simulation and Experimental Validation of Blood Flow in Arteries with Structured-Tree Outflow Conditions *Annals of Biomedical Engineering*; **28**:1281-1299, 2000

[14] Pennati G., Bellotti M., Ferrazzi E., Bozzo M., Pardi G., Fumero R., Blood flow through the ductus venosus in human fetus: calculation using Doppler velocimetry and computational findings, *Ultrasound in Med. and Biol.*;**24**(4):477-487, 1998.

[15] Pennati G., Redaelli A., Bellotti M., Ferrazzi E., Computational analysis of the ductus venosus fluid-dynamics based on Doppler measurements, *Ultrasound in Med. and Biol.*;**22**(8):1017-1029, 1996.

[16] Perktold K., Hofer M., Rappitsch G., Loew M., Kuban B.D., Friedman M.H., Validated computation of physiologic flow in a realistic coronary artery branch,*J. Biomech.*; **31** Mar(3):217-28.1998

[17] Ponzini R., Lemma M., Morbiducci U., Antona C., Montevecchi F., Redaelli A., Doppler derived quantitative flow estimate in coronary artery bypass graft: a computational multi-scale model for the evaluation of the current theory. Submitted, 2006.

[18] Porenta G., Schima H., Pentaris A., Tsangaris S., Moertl D., Probst P., Maurer G., Baumgartner H., Assessment of coronary stenoses by Doppler wires: a validation study using in vitro modeling and computer simulations. *Ultrasound Med Biol.*; **25** (5):793-801, 1999 .

[19] Quarteroni A., Valli A., *Numerical Approximation of Partial Differential Equations*, Springer, 1994.

[20] Redaelli A., Boschetti F., Inzoli F. The assignement of velocity profiles in finite element simulations of pulsatile flow in arteries *Comput. Biol. Med.* **27**(3):233-247, 1997.

[21] Robertson M. B., Khler U., Hoskins P. R., Marshall I., Flow in Elliptical Vessels Calculated for a Physiological Waveform *Journal Of Vascular research* ; **38**:73-82, 2001.

[22] Savader S.J., Lund G.B., Osterman F.A., Volumetric evaluation of blood flow in normal renal arteries with a Doppler flow wire: a feasibility study *Journal of Vascular and Interventional Radiology*; **8**(2): 209-214, 1997.

[23] Sheada R.E., Cobbold R.S., Johnston K.W.,Aarnink R. Three-dimensional display of calculated velocity profiles for physiological flow waveforms. *J. Vasc. Surg.* **17**(4):656-60, 1993.

[24] Veneziani A., Vergara C., Flow rate defective boundary conditions in haemodinamics simulations, *Int. Journ. Num. Meth. Fluids*; **47**, 803-816, 2005.

[25] Veneziani A., Vergara C., An approximate method for solving incompressible Navier-Stokes problem with flow rate conditions. Submitted, 2005.

[26] Viedma A., Jimnez-Ortiz C. and Marco V., Extended Willis Circle model to explain clinical observations in periorbital arterial flow,*Journal of Biomechanics*; **30** (3): 265272, 1997.

[27] Weiman A.E., *Principles and Practice of echocardiography* (second edition), Lea & Febiger, 1994.

[28] Wells R., Syndromes of hyperviscosity, *N. Engl. J. Med.*; **283** (4):183-186, 1970.

[29] F. White, *Viscous Fluid Flow*, McGraw Hill, NY, 1987

[30] RA. Wolthuis, VF. Froelicher Jr, J. Fischer and JH. Triebwasser, The response of healthy men to treadmill exercise *Circulation*; **55**:153-157, 1977.

[31] Womersley J.R., Method for the calculation of velocity, rate of flow and viscous drag in arteries when the pressure gradient is known,*J Physiol.*;**127**(3):553-63,1955.